

Flow Behavior in the Three-Phase Internal-Loop Airlift Reactor with Large Gas Recirculation through the Downcomer

W. Jianping*, J. Xiaoqiang, CH. Xianrui, and Y. Peng

School of Chemical Engineering and Technology,
Tianjin University, Tianjin 300072, China

Original scientific paper

Received: November 11, 2004

Accepted: April 1, 2005

Liquid velocity, gas holdup and solid holdup in the riser and the downcomer of the gas-liquid-solid three-phase internal-loop airlift reactor with large gas recirculation through the downcomer were investigated. A dynamic model for the description of flow behavior in the three-phase internal-loop airlift reactor with large gas recirculation through the downcomer was developed. The model simulates liquid velocity, gas holdup and solid holdup in the riser and the downcomer with satisfactory accuracy.

Keywords:

Airlift reactors, three-phase, fluid dynamics, modeling

Introduction

Gas-liquid-solid three-phase internal-loop airlift reactors, characterized by a well defined flow pattern, better dispersing effects, a higher mass transfer coefficient, a lower gas requirement of complete suspension of the solid, elimination of dead volumes and rapid mixing, are widely used in chemical engineering and petrochemical engineering, especially in biochemical engineering, such as fermentation, waste water purification, hydrogenation and exhaust-gas treatment as well as a large number of gas-liquid-solid three-phase reaction in various process industries.¹⁻⁴ In three-phase internal-loop airlift reactors, the hydrodynamics may play an important role in the performances of these reactors; both experimental and theoretical studies on the flow behavior are necessary parts of any design or evaluation strategy.

Several investigators have studied the hydrodynamics of three-phase internal-loop airlift reactors. *Karamanev* et al.⁵ used 3 mm soft polyurethane foam particles in their experiments. They found that the gas holdup decreased significantly with increasing solids loading and the gas holdup was proportional to $J_G^{1.2}$. *Miyahara* and *Kawate*⁶ measured the gas holdup in the riser and the downcomer, and the pressure drop at the upper and lower ends of the riser due to flow reversal for a solid-suspended airlift reactor containing low-density particles. Based on the measurements, they proposed the empirical correlations between the gas holdup in the riser and the downcomer as well as the pressure drop and the liquid velocity based on the draught tube. *Lu* and

*Hwang*⁷ reported that the liquid velocity did not show any significant variations with top clearance, the liquid velocity increased with an increase in aeration rate or draught tube length and with the decrease in the diameter of the particles, the liquid velocity and the gas holdup decreased with increasing solids loading.

Several models have been developed to describe satisfactorily the hydrodynamics of gas-liquid-solid three-phase airlift reactors. *Miyahara* and *Kawate*⁶ used a simple energy balance to predict the fluid velocity in an internal-loop airlift reactor containing low-density particles. The agreement between the calculated and the measured data was good; however, correlations for the gas holdup and pressure drop must be used in this model. *Vunjak-Novaković* et al.⁸ and *Lu* and *Hwang*⁷ extended the two-phase drift-flux model to analyze the fluid and particle dynamics in a three-phase internal airlift reactor. They found that this model overestimated the liquid velocity. This might be due to the omission of the pressure loss at the top and bottom connecting sections of the airlift reactors in their model. *Livingston* and *Zhang*⁹ extended the two-phase model of *Chisti* et al.,¹⁰ with their assumption of no gas in the downcomer, to predict the liquid velocity and reactor stalling in three-phase airlift reactor. They used a pseudo-homogeneous-phase density for the liquid-solid phase, and took into account the uneven distributions of the solids between the riser and downcomer. *Heijnen* et al.¹¹ have developed a model based on a momentum balance to simulate data measured in large-scale reactors with high gas recirculation through the downcomer. They have assumed a constant ratio between gas holdup in the riser and downcomer and an average solid holdup along the reactor in order to solve the momentum

*Corresponding author. Tel & Fax: +86-22-23501622;
E-mail address: jipwen@tju.edu.cn

balance. *E. García-Calvo et al.*¹² and *M. Tobajas et al.*¹³ have proposed a simple dynamic model based on an energy balance, which took into account the dissipation of energy in the phase interfaces. Their model predicted well when there was little gas recirculation of the downcomer. However, their assumption of no gas in the downcomer is not realistic and then cannot predict well with large gas recirculation through the downcomer at high superficial gas velocities. Moreover, little information is available about the flow behavior of the three-phase internal-loop airlift reactors with large gas recirculation through the downcomer.

The objective of this study was to perform experiments to obtain the hydrodynamic behavior, such as liquid velocity, gas holdup and solid holdup in the riser and downcomer of the gas-liquid-solid three-phase internal-loop airlift reactor with large gas recirculation through the downcomer with low density solid particles. The effects of operating parameters including superficial gas velocity, draught tube cross-sectional area fraction, and solid loading, were investigated. Based on an energy balance, which takes into account the energy input during the gas expansion dissipated in the phase flow and in the phase interfaces, a fluid dynamic model for three-phase internal-loop airlift reactors with large gas recirculation through the downcomer was also developed to predict the liquid velocity, gas holdup and solid holdup in the riser and downcomer.

Theory

Fluid dynamic model

The fluid dynamic model for three-phase internal-loop airlift reactors with large gas recirculation through the downcomer is based on an energy balance, which takes into account that the energy input during the gas expansion is dissipated in the phase flow and in the phase interfaces:

$$E = E_F + E_W + E_S \quad (1)$$

where E is the energy input rate, E_F the energy dissipation due to the net flow, E_W the energy dissipation due to turbulent movement and E_S the energy dissipation at the gas-liquid interface.

For three-phase internal-loop airlift reactors with large gas recirculation through the downcomer, the effect of the solid phase on the average densities in riser and downcomer is considered. It is assumed that there are two different pseudo-homogeneous phases in both reactor sections:

$$\begin{aligned} \rho_M J_G \ln \left(1 + \rho_{HR} \frac{gH}{p_{at}} \right) &= \frac{1}{2} \left[\alpha K_{FR} \rho_{HR} \left(\frac{A_D}{A_R} \right)^2 + \right. \\ &+ \left. K_{FD} \rho_{HD} \right] \frac{A_D}{A_R} \cdot (1 - \varepsilon_{SD} - \varepsilon_{GD})^3 v_{LD}^3 + \\ &+ \frac{0.64 \cdot (2)^{3N/2} N^3 \rho_{HR} F(v_{LO} - v_{LR})^3}{D_R} \cdot \left[\frac{1}{2(3N-1)} + \frac{1}{3N+1} - \frac{2^{1/2}}{3N} \right] + \\ &+ (\varepsilon_{GR} \rho_{HR} + \varepsilon_{GD} \rho_{HD}) u_S gH \end{aligned} \quad (2)$$

Assuming uniform distribution of gas and solid within the riser and the downcomer:

$$\rho_{HR} = \rho_L (1 - \varepsilon_{GR} - \varepsilon_{SR}) + \rho_S \varepsilon_{SR} + \rho_G \varepsilon_{GR} \quad (3)$$

$$\rho_{HD} = \rho_L (1 - \varepsilon_{GD} - \varepsilon_{SD}) + \rho_S \varepsilon_{SD} + \rho_G \varepsilon_{GD} \quad (4)$$

and, taking into account of the momentum balance, proposed by *Livingston and Zhang*,⁹

$$\begin{aligned} \left[(\varepsilon_{GR} - \varepsilon_{GD}) - \left(\frac{\rho_S}{\rho_L} - 1 \right) (\varepsilon_{SR} - \varepsilon_{SD}) \right] gH \rho_L &= \\ = \frac{1}{2} \left[\alpha K_{FR} \rho_{HR} \left(\frac{A_D}{A_R} \right)^2 + K_{FD} \rho_{HD} \right] (1 - \varepsilon_{SD} - \varepsilon_{GD})^2 v_{LD}^2 \end{aligned} \quad (5)$$

The relation of gas holdup in the riser with the liquid velocities and gas slip velocity can be written as:¹⁴

$$\varepsilon_{GR} = \frac{J_G}{u_S + 0.5 v_{LC} + v_{LR}} \quad (6)$$

where v_{LC} is calculated by taking into account the parabolic profile of the liquid velocity in the riser and all other assumptions described there. After calculation for three-phase system the following equation is obtained:

$$v_{LC} = \frac{(v_{LD} - v_{LR})}{(1 - \varepsilon_{GR} - \varepsilon_{SB})} \left(\frac{N}{N+2} \right) \quad (7)$$

A gas-phase volume balance at the riser bottom equates the riser gas flow rate to the sum of the downcomer gas flow rate and the injection gas flow rate (at the riser bottom):

$$v_{GR} \varepsilon_{GR} A_R = v_{GD} \varepsilon_{GD} A_D + A J_G \quad (8)$$

or

$$(v_{LR} + u_{SGR}) \varepsilon_{GR} A_R = (v_{LD} - u_{SGD}) \varepsilon_{GD} A_D + A J_G \quad (9)$$

where u_{SGR} and u_{SGD} are the gas slip velocities in riser and downcomer and J_{GM} is the superficial gas velocity based on the total cross-sectional area and the injection gas flow rate. With the simplifying assumption $u_{SGR} = u_{SGD} = u_S$ (gas slip velocity), Eq. (9) becomes:

$$(v_{LR} + u_S)\varepsilon_{GR}m = (v_{LD} - u_S)\varepsilon_{GD}(1 - m) + J_G \quad (10)$$

in which m is the draught tube cross-sectional area fraction:

$$m = \frac{A_S}{A} \quad (11)$$

The liquid-phase balance is:

$$v_{LR}A_R(1 - \varepsilon_{GR} - \varepsilon_{SR}) = v_{LD}A_D(1 - \varepsilon_{GD} - \varepsilon_{SD}) \quad (12)$$

For the overall gas holdup ε_G :

$$\varepsilon_G = m\varepsilon_{GR} + (1 - m)\varepsilon_{GD} \quad (13)$$

Following the criteria of *Livingston* and *Zhang*⁹ the fraction of the total solid in the riser and the downcomer can be calculated as a ratio between the time taken by the particles to travel through the riser and the total time taken for the particle to travel through a complete loop. It can be written in relation to the liquid and solid velocities as:

$$f_R = \frac{v_{LD} + u_t}{v_{LD} + v_{LR}} \quad (14)$$

The solid fraction in the downcomer is easily calculated by knowing that $f_R + f_D = 1$. The fractional solid holdup in the riser and the downcomer can be calculated from Eq. (14) and defining the ε_S^0 ($\varepsilon_S^0 = \varepsilon_S/m$) as the solid holdup in the riser when all the particles are there:

$$\varepsilon_{SR} = \varepsilon_S^0 \frac{v_{LD} + u_t}{v_{LD} + v_{LR}} \quad (15)$$

$$\varepsilon_{SD} = \varepsilon_S^0 \frac{A_R}{A_D} \frac{v_{LR} - u_t}{v_{LD} + v_{LR}} \quad (16)$$

hence,

$$\varepsilon_S = m\varepsilon_{SR} + (1 - m)\varepsilon_{SD} \quad (17)$$

Parameters estimation

In order to apply the described model, geometrical parameters and solid and liquid characteristics can be easily obtained in any case. N is assumed as 2.¹² Friction coefficients, K_{fR} and K_{fD} , particle settling velocities and slip gas velocities are estimated following an independent methodology.

Friction coefficients, K_{fR} and K_{fD}

The K_{fi} are calculated using the Fanning equation:

$$K_{fi} = 4f \frac{L_i}{D_i} \text{ for } i = R \text{ or } D \quad (18)$$

and the friction factors obtained from the Blasius equation for one-phase flow:

$$f = 0.0791 Re_{Hi}^{-0.25} \quad (19)$$

$$Re_{Hi} = \frac{\rho_{Hi} v_{Li} D_i}{\mu_{Hi}} \quad (20)$$

The pseudohomogeneous density ρ_{Hi} was calculated using Eqs. (3) and (4), and the apparent viscosity μ_{Hi} was calculated by using the Oliver equation:¹⁵

$$\mu_{Hi} = \mu_{li} \frac{(1 - 0.75\varepsilon_S^{1/3})(1 - 2.15\varepsilon_S)}{(1 - \varepsilon_S)^2} \quad (21)$$

The presence of gas introduces variation in the friction coefficients in relation to the homogeneous one-phase flow,¹⁶ K_{fR} is multiplied by the α parameter to take into account the presence of the gas phase. For $N = 2$, α is also 2.^{12,17}

Particle settling velocity

Di Felice et al. proposed a semi-empirical equation to calculate u_t of solid particles in a liquid as a function of $u_{t\infty}$.¹⁸ Following the assumptions made by *Di Felice* et al. and taking into account the presence of gas, the following equation is obtained:

$$u_t = u_{t\infty} \varepsilon_L (1 - \varepsilon_S) \left(\frac{2 - \varepsilon_S}{2} \right)^{0.5} \quad (22)$$

A great number of correlations estimate the settling velocity of a single particle in stagnant fluid, known terminal settling velocity ($u_{t\infty}$). By Stoke's law,

$$u_{t\infty} = \frac{g d_S^2 (\rho_S - \rho_L)}{18\mu_L} \quad (23)$$

Slip gas velocity

The slip velocity was calculated by using the equation proposed by *Wilkinson* for non-coalescent systems:¹⁹

$$\frac{u_S u_L}{\sigma} = 2.25 \left(\frac{\sigma^3 \rho_L}{g \mu_L^4} \right)^{-0.273} \left(\frac{\rho_L}{\rho_G} \right)^{0.03} \quad (24)$$

The value of slip gas velocity is $0.25 \text{ m}\cdot\text{s}^{-1}$ for air-water system.

Model solution

Liquid velocity in the downcomer is the first parameter to be calculated in this model. The algorithm for the predictions of the liquid velocity in the downcomer is shown in Fig. 1.

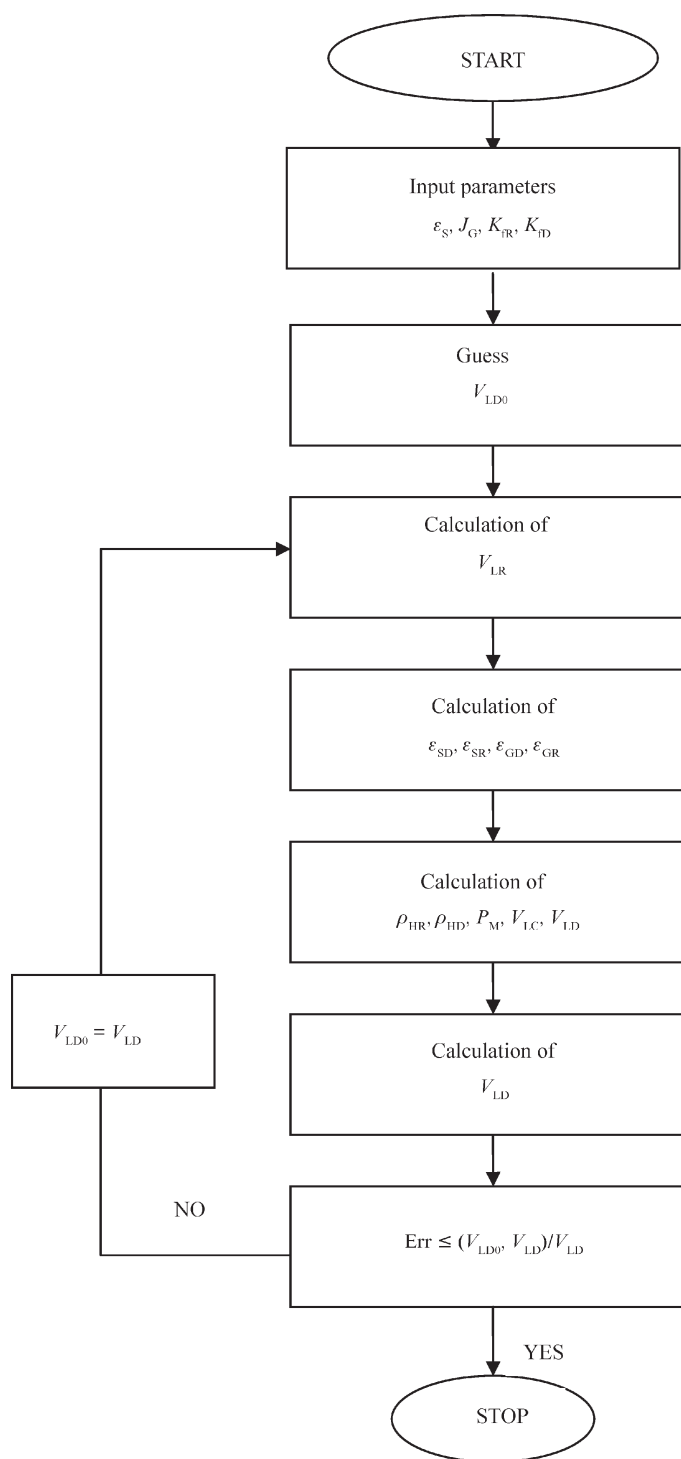


Fig. 1 – Algorithm for the prediction of the liquid velocity in the downcomer

Experimental

Apparatus

The internal-loop airlift reactor was constructed of $D_{in} = 0.12 \text{ m}$ Plexiglas column $h = 1.2 \text{ m}$ in height. At the top of the reactor was installed an expander of $D_{in} = 0.16 \text{ m}$ and $h = 0.24 \text{ m}$ height. The height of the draft tube was 0.9 m and was 0.15 m above the bottom of the reactor. The inside diameter of draft tube was $0.08, 0.085$ and 0.09 m (wall thickness 0.001 m); accordingly, $m = 0.44, 0.50$ and 0.56 , respectively. The distance between the liquid surface free of air and the upper end of the draft tube was 0.10 m . The diameter of the concentric jet nozzle is 0.0054 m , and located at 0.075 m below the draft tube. The gas flow rate was controlled by a mass flowmeter.

Materials

Water and air were used as the liquid and gas phase in all the experiments, and the gas flow rate was varied in a way that the superficial gas velocity were between 0.06 and $0.15 \text{ m}\cdot\text{s}^{-1}$ so that there was large gas recirculation in the downcomer. Plastic beads with the diameter of approximately 2 mm and the density of $1340 \text{ kg}\cdot\text{m}^{-3}$ were used as solid phase. Different particles volume of $150, 450$ and 750 ml were put into the system; accordingly, the solid loadings were $\varphi = 1.1 \%, 3.3 \%$ and 5.5% , respectively.

Methods

Liquid velocity

The liquid velocity in the riser and downcomer were obtained by four pH sensors located in the riser and downcomer sections, two in each section. The response time of the pH sensors is 0.1 s . The signals of all pH sensors were transmitted to a computer by an A/D and D/A data acquisition system. The pH values of the liquid in the riser and downcomer sections were recorded every 0.1 s by the computer. The computer recording was synchronized manually with the introduction of every pulse of $1 \text{ ml } 10 \text{ mol}\cdot\text{l}^{-1}$ NaOH solution through the injection port located at 0.05 m above the bottom of the reactor. Then, the liquid linear velocities in the riser and downcomer are obtained by the following equations:

$$v_{LR} = \frac{L_R}{t_R} \quad (25)$$

$$v_{LD} = \frac{L_D}{t_D} \quad (26)$$

where L_R and L_D are the distances between the two pH sensors in the riser and downcomer, respectively, and t_R and t_D are the average differences in response time of the second and third peaks of the response curves obtained by the two pH sensors in the riser and downcomer, respectively. Note, that the second and third peaks of the response curves are used to obtain t_R and t_D , because the first peak of the response curve obtained by the lower pH sensor in the riser is not well-established at a higher aeration rate.²⁰

Gas holdup

Gas holdups in the riser and downcomer were obtained by 5-point conductivity probe located at 0.7 m above the bottom of this reactor, respectively.

Solid holdup

The solid holdup in the riser and the downcomer was estimated by a momentum balance over an element of the riser or the downcomer (dz).²¹

$$\epsilon_S = \frac{\rho_L}{\rho_S - \rho_L} \left(\frac{dh_{Bi}}{dz} - \frac{dh_i}{dz} \right) \quad (27)$$

where dh_{Bi} is the manometric difference in two-phase mode and dh_i in three-phase system. Four U-type manometers were allowed to obtain the head loss due to the flow by measuring the manometric difference.

Result and discussion

Effects of the operating parameters

Effect of superficial gas velocity (J_G)

At the fixed solid loading ($\epsilon_S = 3.3\%$), the effect of superficial gas velocity, Figure (J_G) on the hydrodynamic behavior such as the liquid velocity in the riser (v_{LR}) and the downcomer (v_{LD}), the gas holdup in the riser (ϵ_{GR}) and the downcomer (ϵ_{GD}), and the solid holdup in the riser (ϵ_{SR}) and the downcomer (ϵ_{SD}), are shown in Figure 2–4. The variable points represented the experimental data and the different lines represented the simulated results by the proposed model. From Figure 2, it can be seen that v_{LR} and v_{LD} increase with increasing J_G , ϵ_{GR} and ϵ_{GD} increase with increasing J_G , as shown in Figure 3, similar results were also reported by *Lo* and *Hwang*.²² Figure 4 shows the Effect of J_G on ϵ_{SR} and ϵ_{SD} at the fixed solid loading, ϵ_{SR} decreases with increasing J_G , but ϵ_{SD} increases with increasing J_G .

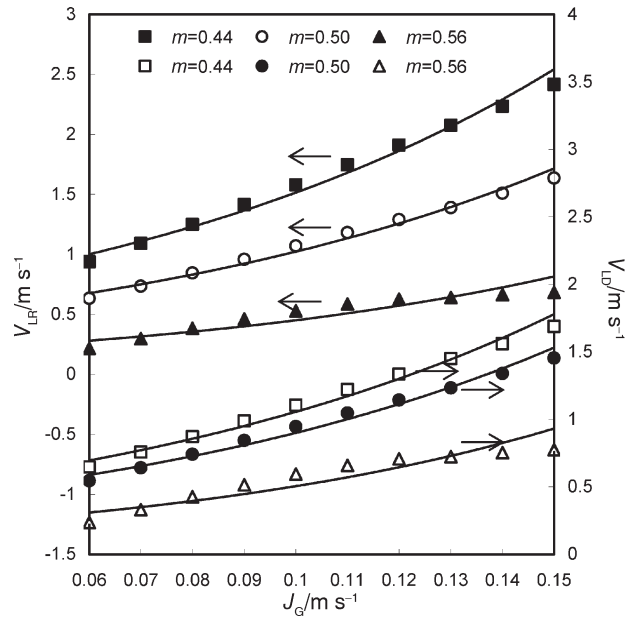


Fig. 2 – Effects of J_G and m on the liquid velocity in the riser and downcomer

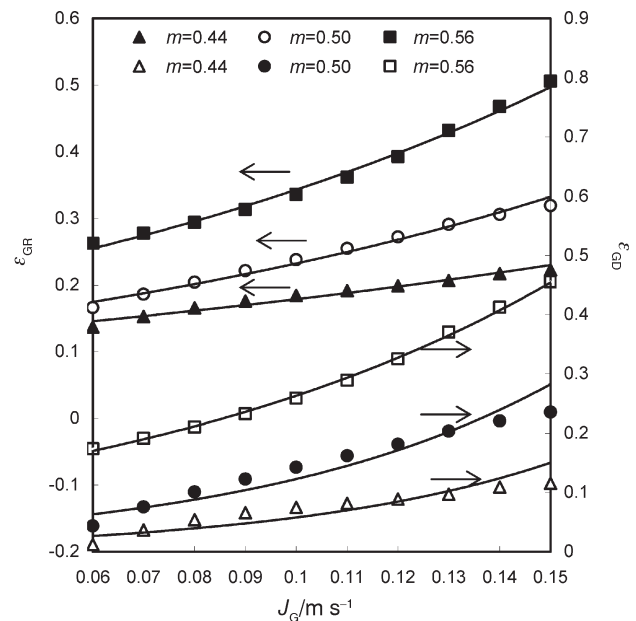


Fig. 3 – Effect of J_G and ϵ_S on the gas holdup in the riser and downcomer

Effect of draught tube cross-sectional area fraction (m)

Figure 2–4 also show the Effect of draught tube cross-sectional area fraction (m) on the liquid velocity in the riser (v_{LR}) and the downcomer (v_{LD}), the gas holdup in the riser (ϵ_{GR}) and the downcomer (ϵ_{GD}), and the solid holdup in the riser (ϵ_{SR}) and the downcomer (ϵ_{SD}) at the fixed solid loading ($\epsilon_S = 3.3\%$). As shown in the figure, v_{LR} and v_{LD} de-

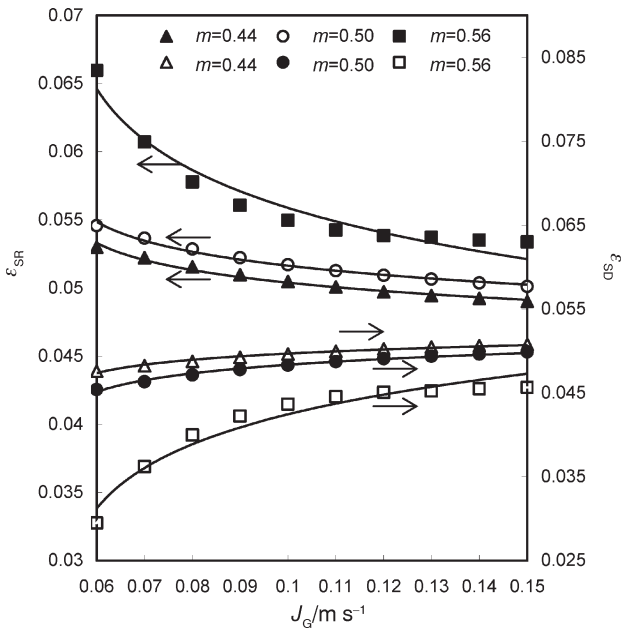


Fig. 4 – Effect of J_G and ϵ_S on the solid holdup in the riser and downcomer

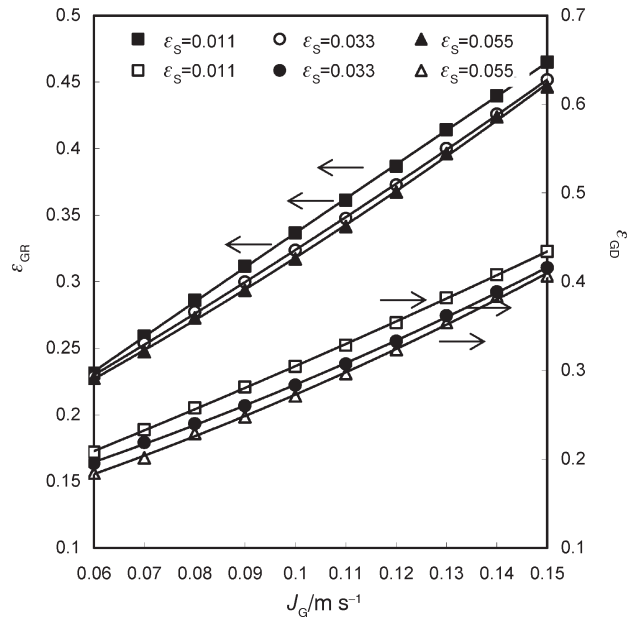


Fig. 6 – Effect of J_G and ϵ_S on the gas holdup in the riser and downcomer

crease with increasing m from the value of 0.44 to 0.56 in this reactor. Contrarily, ϵ_{GR} and ϵ_{GD} increase with increasing m . Figure 4 shows the Effect of m on ϵ_{SR} and ϵ_{SD} at the fixed solid loading, ϵ_{SR} increases with increasing m , but ϵ_{SD} decreases with increasing m from the value of 0.44 to 0.56 in this reactor.

Effect of solid loading (ϵ_S)

Figure 5–7 show the Effect of solid loading (ϵ_S) on the liquid velocity in the riser (v_{LR}) and the

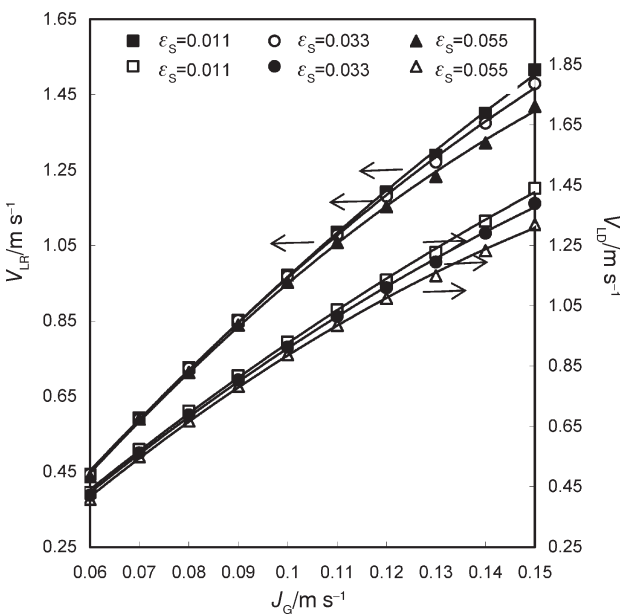


Fig. 5 – Effect of J_G and ϵ_S on the liquid velocity in the riser and downcomer

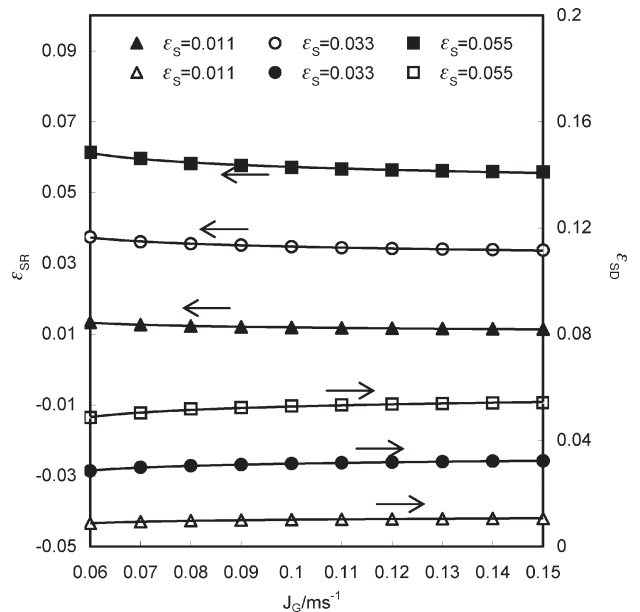


Fig. 7 – Effect of J_G and ϵ_S on the solid holdup in the riser and downcomer

downcomer (v_{LD}), the gas holdup in the riser (ϵ_{GR}) and the downcomer (ϵ_{GD}), and the solid holdup in the riser (ϵ_{SR}) and the downcomer (ϵ_{SD}) at the fixed cross-sectional area fraction of the riser to the reactor ($m = 0.50$). As shown in these figures, v_{LR} and v_{LD} decrease with increasing ϵ_S . Similarly, ϵ_{GR} and ϵ_{GD} decrease with increasing ϵ_S . Contrarily, ϵ_{SR} and ϵ_{SD} increase with increasing ϵ_S .

Comparison between experimental data and model prediction

Figure 8–10 show the experimental and calculated values of liquid velocity, gas holdup and solid holdup in the riser and the downcomer, respectively, in a wide range of operating conditions such as the superficial gas velocity, cross-sectional area fraction of the riser to the reactor and solid loading. It can be seen that differences between experimental and predicted values are lower than 20 % in most cases. Then the simulated results agree well with the experimental data. The pro-

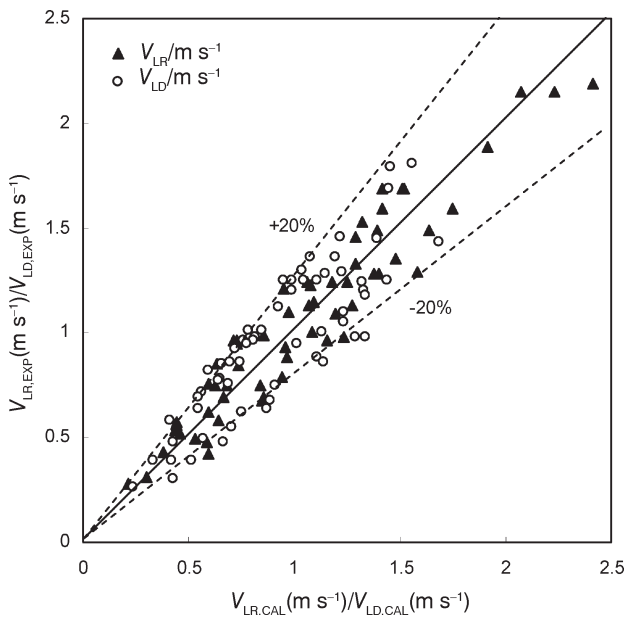


Fig. 8 – Comparison between calculated and experimental liquid velocity in the riser and downcomer

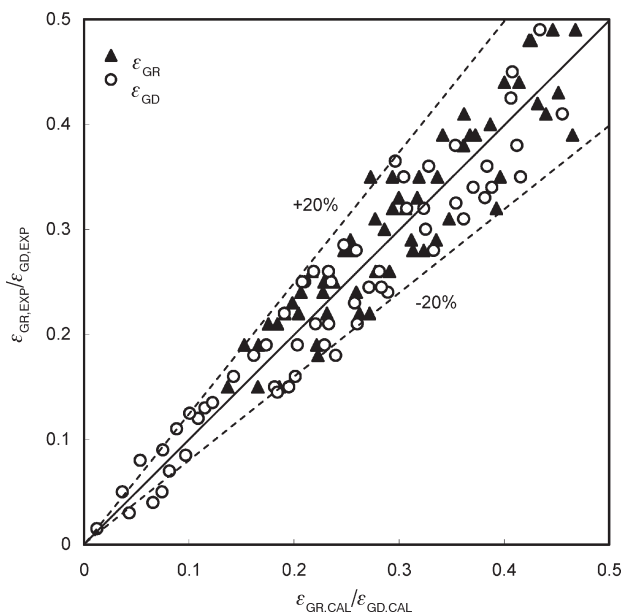


Fig. 9 – Comparison between calculated and experimental gas holdup in the riser and downcomer

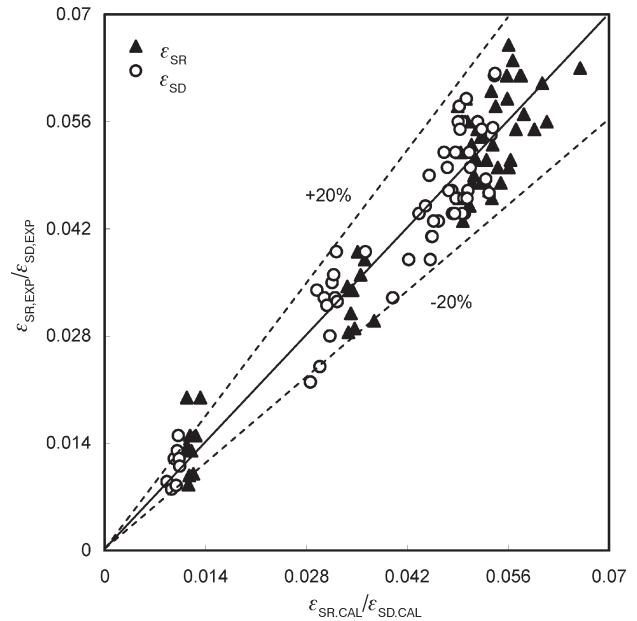


Fig. 10 – Comparison between calculated and experimental solid holdup in the riser and downcomer

posed model is capable of predicting the fluid dynamic parameters of three-phase internal-loop airlift reactor with large gas circulation through the downcomer.

Conclusions

(1) Experiments were conducted to investigate the liquid velocity, gas holdup and solid holdup in the riser and downcomer of the three-phase internal-loop airlift reactor with large gas circulation through the downcomer. It was found that v_{LR} , v_{LD} , ϵ_{GR} , ϵ_{GD} and ϵ_{SD} increase with the increase in J_G , but ϵ_{SR} decreases with the increase in J_G ; ϵ_{GR} , ϵ_{GD} and ϵ_{SR} increase with the increase in m but v_{LR} , v_{LD} , and ϵ_{SD} decrease with the increase in m ; v_{LR} , v_{LD} , ϵ_{GR} , ϵ_{GD} decrease with the increase in ϵ_S , but ϵ_{SR} and ϵ_{SD} increase with the increase in ϵ_S .

(2) A mathematical model based on an energy balance was proposed to predict the liquid velocity, gas holdup and solid holdup in the riser and downcomer in three-phase internal-loop airlift reactor. Good agreement between the predicted and the measured values of the liquid linear velocity and gas holdup was demonstrated in this study.

ACKNOWLEDGEMENTS

The authors wish to acknowledge the financial support provided by the National Natural Science Foundation of China (No. 20176040, 20336030, 90206001) and the General Corporation of Petrochemical Engineering of China (No. 301014).

Nomenclature

A	– area, m^2
$\frac{A_D}{A_R}$	– downcomer to riser cross-sectional area ratio, –
D	– diameter, m
D_{in}	– inside diameter, m
d_p	– mean particle diameter, mm
E	– energy input, $W \cdot m^{-2}$
E_F	– friction losses between liquid and device, $W \cdot m^{-2}$
f	– friction factor, –
g	– gravitational acceleration, $m \cdot s^{-2}$
H	– liquid height, m
h	– height, m
J_G	– superficial gas velocity, $m \cdot s^{-1}$
K_f	– friction factor, –
L_S	– equivalent length, m
m	– the draught tube cross-sectional area fraction, –
N	– liquid velocity profile parameter, –
p	– pressure, Pa
E_S	– friction losses at the liquid-gas interface, $W \cdot m^{-2}$
u_S	– gas slip velocity, $m \cdot s^{-1}$
u_t	– settling velocity of solid particles, $m \cdot s^{-1}$
v_G	– gas velocity, $m \cdot s^{-1}$
v_{LO}	– linear velocity in the axial axis of column, $m \cdot s^{-1}$
v_{LC}	– average velocity in the core region, $m \cdot s^{-1}$
E_W	– friction losses due to internal recirculation, $W \cdot m^{-2}$

Greek letters

α	– parameter related to two-phase flow, –
ε	– holdup, –
ε_S^0	– total solid holdup referred to the volume of the riser, –
μ	– viscosity, $kg \cdot m^{-1} \cdot s^{-1}$
ρ	– density, $kg \cdot m^{-3}$
φ	– volume fraction, %
σ	– strain, Pa

Subscripts

D	– downcomer
G	– gas
H	– pseudo-homogeneous

L	– liquid
M	– middle
R	– riser
S	– solid

References

1. Douek, R. S., Livingston, A. G., Johanson, A. C., Hewitt, G. F. I., *Chem. Eng. Sci.* **49** (1994) 3719.
2. Srinivasulu, B., Prakasham, R. S., Jetty, A., Srinivas, S., Ellaiyah, P., Ramakrishna S. V., *Process Biochem.* **38** (2002) 593.
3. Wang, T. F., Wang, J. F., Yang, W. G. Jin Y., *Powder Technol.* **137** (2003) 83.
4. Quan, X. C., Shi, H. C., Zhang, Y. M. Wang, J. L., Qian, Y., *Sep. Purif. Technol.* **34** (2004) 97.
5. Karamanev, D. G., Nagamune, T., Endo, I., *Chem. Eng. Sci.* **47** (1992) 3581.
6. Miyahara, T., Kawate, O., *Chem. Eng. Sci.* **48** (1993) 127.
7. Lu, W. J., Hwang, S. J., Chang, C. M., *Chem. Eng. Sci.* **50** (1995) 1301.
8. Vunjak-Novaković, G., Jovanović, G., Kundaković, L., Obradović, B., *Chem. Eng. Sci.* **47** (1992) 3451.
9. Livingston, A. G., Zhang, S. F., *Chem. Eng. Sci.* **48** (1993) 1641.
10. Chisti, Y., Hallard, B., Moo-Young, M., *Chem. Eng. Sci.* **43** (1988) 451.
11. Heijnen, J. J., Hols, J., van der Lans, van Leeuwen R. G. J. M., Mulder, A., Weltevrede, R., *Chem. Eng. Sci.* **52** (1997) 2527.
12. García-Calvo, E., Rodriguez, A., Prados, A., Klein, J., *Chem. Eng. Sci.* **54** (1999) 2359.
13. Tobajas M, García-Calvo E, Siegel M H, Apitz S. E., *Chem. Eng. Sci.* **54** (1999) 5347.
14. García-Calvo, E., Letón, P. *Chem. Eng. Sci.* **46** (1991) 2947.
15. Oliver, D. R., *Chem. Eng. Sci.* **15** (1961) 230.
16. Hsu, Y.C., Dudukovic, M.P., *Chem. Eng. Sci.* **35** (1980) 135.
17. García-Calvo, E., *A.I.Ch.E. J.* **38** (1992) 1662.
18. Di Felice, R., Gibilaro, L. G., Foscolo, P. U., *Chem. Eng. Sci.* **18** (1995) 3005.
19. Wilkinson, P. M., Ph.D. thesis, Groningen, Netherlands, 1981.
20. Lu, W. J., Hwang, S. J. Chang, C. M. *Chem. Eng. Sci.* **49** (1994) 1465.
21. Epstein, N., *Can. J. Chem. Eng.* **59** (1981) 649.
22. Lo, C. S., Hwang S. G., *Chem. Eng. J.* **91** (2003) 3.